477801

Update on the Greenland Ice Sheet Melt Extent: 1979-1999

Waleed Abdalati
Laboratory for Hydrospheric Processes
NASA Goddard Space Flight Center
Code 971
Greenbelt, MD 20771

Konrad Steffen ??
Cooperative Institute for Research in Environmental Sciences
Campus Box 216
University of Colorado
Boulder, Colorado 80309

For submission to *Journal of Geophysical Research Atmospheres*, July, 2000

Abstract

Analysis of melt extent on the Greenland ice sheet is updated to span the time period 1979-1999 is examined along with its spatial and temporal variability using passive microwave satellite data. In order to acquire the full record, the issue of continuity between previous passive microwave sensors (SMMR, SSM/I F-8, and SSM/I F-11), and the most recent SSM/I F-13 sensor is addressed. The F-13 XPGR melt-classification threshold is determined to be –0.0154. Results show that for the 21-year record, an increasing melt trend of nearly 1 %/yr is observed, and this trend is driven by conditions on in the western portion of the ice sheet, rather than the east, where melt appears to have decreased slightly. Moreover, the eruption of Mt. Pinatubo in 1991 is likely to have had some impact the melt, but not as much as previously suspected. The 1992 melt anomaly is 1.7 standard deviations from the mean. Finally, the relationship between coastal temperatures and melt extent suggest an increase in surface runoff contribution to sea level of 0.31 mm/yr for a 1°C temperature rise.

Introduction

Understanding the Greenland ice sheet melt characteristics is critical to the assessment of ice sheet mass balance and the interpretation of the mass balance observations. Because of the positive albedo feedback associated with snow melt and the fact that wet snow absorbs as much as three times more incident solar energy than dry snow, ice sheet melt characteristics play a major role in the energy and mass exchanges at the ice sheet surface. Moreover, surface melt can act to enhance the flow of outlet glaciers through crevasse overdeepening [Robin, 1974; van der Veen, 1998] and is believed to have contributed to the very rapid thinning of a number of outlet glacier in Eastern Greenland [Krabill et al., 1999]. As a result, not only is ice sheet melt directly tied to ablation through surface evaporation and runoff, but it is indirectly linked to discharge through its potential contributions to discharge rates.

Detection of surface melt at large spatial scales is most effectively accomplished through the use of satellite microwave data, which has a clear melt signature that arises from the transition from volume- to surface-scattering during melt onset [Mätzler and Hüppi, 1989]. As such, wet-snow emission approaches black body behavior, and this change in emission characteristics is detectable by most microwave sensors at frequencies in excess of 10 GHz. [Ulaby et al., 1986]. These changes in emission characteristics have formed the basis of several passive-microwave-based melt assessment algorithms [Mote et al., 1993; Mote and Anderson, 1995; Zwally and Fiegles, 1995; Abdalati and Steffen, 1995,;Abdalati and Steffen, 1997]. These algorithms are all applicable to Scanning Multi-channel, Microwave Radiometer (SMMR) and Special Sensor Microwave/Imager (SSM/I) instruments, which have provided near-continuous of coverage since October, 1978.

Melt can be retrieved at higher spatial resolution by other sensors that operate in the visible part of the electromagnetic spectrum; however, SMMR and SSM/I instruments offer the advantage that they are not strongly affected by cloud cover at the lower frequencies, and their wide swath provides frequent coverage of the high-latitude regions – several times a day in the case of Greenland. In addition, the melt signature is not as distinct at visible wavelengths as it is in the microwave. Based on these characteristics, plus the fact that there is a consistent microwave record covering the last 21 years, the SMMR and SSM/I time series are best suited for such studies.

Recent analyses [Abdalati and Steffen, 1997a and 1997b] have examined the passive microwave melt record for the ice sheet through 1994 and 1995 respectively utilizing the SMMR, SSM/I F-8, and SSM/I F-11 instruments. These records showed a very dramatic increasing melt trend which appeared to be interrupted by the eruption of Mt. Pinatubo in June, 1991. With effects of Mt. Pinatubo possibly lingering in 1995, it was difficult to determine whether the trend would continue, or the extent to which Pinatubo was anomalous. Since 1995, however, the SSM/I F-11 instrument has been replaced by the F-13 sensor, which has provided data for the past five years. In this paper, we examine the relationships between the SSM/I F-11 and F-13 emission characteristics as they pertain to melt, and determine the appropriate F-13 criterion to yield a consistent extension of the 1979-1999 melt record. We then calculate that record and examine the trends from the longer data set including their spatial character, and re-evaluate the impact of Mt. Pinatubo.

Approach

The method of melt determination used in this study is the cross-polarized gradient ratio (XPGR) approach of Abdalati and Steffen [1997a]. The XPGR is given as:

$$XPGR = [Tb(19h)-Tb(37v)] / [Tb(19h)+Tb(37v)] \quad (1)$$

where Tb(19h) is the 19 GHz horizontally polarized brightness temperature (18 GHz in the case of SMMR) and Tb(37v) is the 37 GHz vertically polarized brightness temperature for both the SMMR and SSM/I instruments. It has been shown that a threshold can be established in the XPGR which allows the classification of wet and dry snow. The basis of the method lies in the fact that the microwave emission melt signature varies with frequency and polarization. The combination of these channels in the XPGR exploits these differences, and further minimizes the effects of differing physical temperatures through normalization [Abdalati and Steffen, 1995].

Daily melt variations have been successfully studied using a 37 GHz horizontal (37h) single-channel approach [Mote and Anderson, 1995], which is particularly well suited for capturing day-to-day surface melt variability. The XPGR technique is a higher inertia signal, however, that is less sensitive variations directly at the surface. As such, it is well suited to seasonal analyses, and is the method used in this study.

For each passive microwave sensor, an XPGR melt-classification threshold is determined. Pixels on the ice sheet with XPGR values in excess of the threshold on a given day are classified as experiencing melt on that day, whereas those with values below the threshold are classified as dry. This criterion was applied to every ice sheet pixel for which there was data during the summer months (June, July, and August) of the 21-year passive microwave record from 1979-1999, and melt extent for each day was determined. These daily values were combined into a mean melt extent for each year for the ice sheet as a whole, and for each of the major topographically-defined climate zones described by Ohmura and Reeh [1991]. The ice mask used was generated from a digitization of the Quaternary map of Greenland (1:250000 scale) produced by the Geological survey of Denmark and is shown in Figure 1. Only pixels fully contained in the ice sheet were used to minimize mixed-pixel effects.

A limitation of this and other satellite-based melt detection techniques is that the results are binary. A pixel can only be classified as wet or dry, and no direct information about the actual ablation amount for each pixel is available. However, the mean melt extent serves as a reasonable proxy for the actual ablation amount.

The passive microwave data used in the melt detection were the polar-stereographic SMMR (1979-1986 melt seasons plus June and July of 1987), SSM/I F-8 (August 1987 plus the 1988-1991 melt seasons), SSM/I F-11 (1992-1994 melt seasons), and SSM/I F-13 (1995-1999 melt seasons). The analysis for 1979 through 1994 was previously completed by Abdalati and Steffen [1997], and a description of the analysis will not be repeated here. The current effort focuses on the SSM/I F-13 years of 1995 through 1999, and also the spatial trends in the melt for each climate zone.

Analysis of the F-13 data requires an adjustment to the XPGR melt threshold to account for various instrument and orbital differences between it and the other sensors. The F-13 characteristics are discussed in relation to other SSM/I instruments by Stroeve et al. [1998]. The SMMR, F-8, and F-11 sensors were all intercalibrated to the F-8 baseline using the coefficients of Jezek et al., [1991] and Abdalati et al. [1995]. Similar consistency must be maintained in this analysis. Fortunately, there is a five-month overlap of data from the F-11 and F-13 instruments from May 3, 1995 through September 30, 1995, spanning the melt period. To cross-calibrate the instruments for consistency in the melt record we first identified the F-11-derived melt pixels for the overlap period. We then calculated the F-13 melt pixels for the same period using thresholds that varied from –0.0100 to –0.0200 in increments of 0.0001. For each F-13 XPGR threshold, we calculated the number of pixels that were mismatched – i.e. classified as wet by one sensor and dry by another. This was done initially for the whole overlap period and again for just the summer melt season. In both cases the differences converged to a minimum at an F-13 melt threshold of –0.0154, which is adopted as the F-13 melt criterion. Because the instruments are nearly identical, and their equatorial crossing times differ by only about 40 minutes, it is encouraging that the XPGR melt threshold only requires only a minor adjustment.

Results and Discussion

The melt extent of the various climate zones, along with the pixels used for each zone are shown in Figure 2. Trends are positive by well over 1%/yr in the four western regions, and close to zero or negative in the eastern regions. As most of the ice sheet melt occurs in the shallow-sloped western flank it is these conditions that dominate the ice sheet melt as a whole. Whereas the east, with its steep slopes, and relatively low melt area is less significant. Trends appear to be strongly negative in the Scoresbysund area, but melt in this vicinity is only about 3% that of the total ice sheet, and the climate conditions are fairly isolated due to the mountainous terrain such that the conditions in this region are of negligible significance as compared to the ice sheet as a whole. Melt in the Tunu area is more expansive comprising approximately 10% of the total melt area. The downward trend in the Tunu area is very small.

The melt extent for the ice sheet as a whole along with the coastal temperature record for the six stations that are shown in Figure 1 is presented in Figure 3. Dominated by conditions in the west, it shows a positive trend of 0.97%/yr of melt. Because of the scatter in annual values, however, the trend is only at the 88% significance level. With the additional five years of data as compared to Abdalati and Steffen [1997] the correlation coefficient between the temperature and the melt increases from R=0.78 to R=0.82 and the spatial melt sensitivity to temperature decreases slightly from 73,000 $km^2/°C$ to 68,000 $km^2/°C$, with the latter likely to be slightly more accurate because of the longer data set and stronger correlation. This melt/temperature sensitivity is also dominated by conditions in the west where slopes are relatively shallow near the melt margins. In these regions, small vertical movements in the zero-degree isotherm results in a more significant horizontal change in melt are then in the east, where slopes are steeper.

Of particularly interest is the apparent effect Mt. Pinatubo eruptions in June, 1991 during which an estimated 20 Mt of sulfur dioxide were ejected into the stratosphere [Bluth et al., 1992]. In the months that followed, this additional atmospheric loading and associated increase in optical thickness had developed with worldwide implications, most notably reduced tropospheric temperatures. Effects of this stratospheric loading were apparent in the 1992 melt signature [Abdalati and Steffen, 1997b], which was significantly reduced as compared to previous years. With the extended record in this study, the 1992 melt season is still the lowest in the record is but is only 1.7 standard deviations from both the mean and the predicted 1992 value based on the trend. This translates to a 90% probability that the 1992 value is outside the natural variability. As such, it is likely that the eruption did affect the melt, but not to the extent previously believed.

Globally, the recovery from Mt. Pinatubo is believed to have occurred by 1995 [Hansen et al., 1996], which is consistent with the estimated e-folding time constant of 500 days reported for mid latitudes [Post et al., 1996]. Assuming this to be the case, if we remove the melt years of 1992, 1993, and 1994, the melt trend increases by nearly half to 1.4 %/year. Stone et al. [1993] suggest that the aerosol decay may occur more slowly in the

Arctic because of the nature of the circulation patterns and vaporization and regrowth processes. The temperatures and melt conditions in Figure 3 suggest that these effects may have lingered on into 1996, in which case the melt trend increases to 2% per year; however, in the absence of studies that support the longer e-folding time for the Arctic, such a conclusion cannot be confidently drawn.

It is interesting to note that the second lowest melt year in the record, follows the eruptions of another major volcano, El Chichon in March and April, 1982. With roughly half the sulfur dioxide input to the atmosphere [McCormick et al., 1984], its global effects are not as dramatic, and it may be of negligible consequence to the melt record, but it is possible that the low melt value for 1982 may have been partially influenced by the eruption. The e-folding time constant for El Chichon was estimated at 208 days [Post et al., 1995], however, so if it is did impact the melt, it's effects would have been nearly 90 % diminished by the following melt season.

Finally, in an attempt to arrive at a coarse estimate of the corresponding melt contribution to sea level rise in a warming climate, we make the following assumptions: 1) the average summer melt extent is 145,000 km^2/yr (calculated from the 21-year passive microwave time series), 2) the surface melt increase is directly proportional to surface ablation and runoff, 3) surface melt and runoff losses are annually 237 km^3 of water per year [Warrick et al., 1996], and 4) a loss of 360 km^3/yr translates to a 1 mm/yr sea level rise. In the case of assumption #2, it is true that when melt area increases, the higher-elevation melt generally percolates into the firn and refreezes, thus not contributing to the mass loss. At the same time, however, melt at the lower elevations is increasing similarly, so we are assuming that the percolation/runoff ratio remains constant. Based on these assumptions, surface runoff associated with a 1°C temperature rise will contribute an additional 0.31 mm/yr to sea level rise above and beyond Greenland's current contribution, minus whatever accumulation increase results from increased temperatures.

These assumptions do not account for enhanced discharge that is likely to occur with the overdeepening of water-filled crevasses. Such overdeepening is an effective means of delivering water to the bed of some of the more temperate outlet glaciers [Robin, 1974; Paterson, 1994], which can lubricate the bedrock/ice interface and increase discharge. It has been suggested that such a mechanism may be responsible for the substantial thinning observed in several of Greenland's southeastern outlet glaciers [Krabill et al., 1999, Abdalati et al., this issue]. These effects are complex and non-linear, and are likely to make the ice sheet contribution to sea level rise significantly greater.

Conclusions

Geophysical parameter matching of melt conditions derived with the SSM/I F-11 and F-13 instruments indicates that the appropriate F-13 XPGR melt-classification threshold is –0.0154. F-13 pixels with XPGR values in excess of this threshold can be classified as wet, whereas those with lower values can be classified as dry. Results for the 21-year time series show an increasing melt trend of 1 %/yr at the 88% significance level. This

trend is strongly driven by conditions on in the western portion of the ice sheet, rather than the east, where melt appears to have decreased slightly. The correlation coefficient between coastal temperatures and ice sheet melt is 0.82 and the associated relationship between warming in Greenland and increased melt is such that a 1°C temperature rise is expected to result in a 68,000 km increase in melt area (or 47%). The resulting relationship between surface runoff and sea level rise is estimated to be 0.31 mm/yr for a 1°C temperature increase.

The eruption of Mt. Pinatubo in 1991 is likely to have had some impact the melt, but not as much as previously suspected, as the 1992 melt anomaly is 1.7 standard deviations from the mean. Elimination of the 3 post-Pinatubo years indicates a stronger trend of 1.4 %/yr. There is a quasi-periodic character to the ice sheet melt extent on the order of several years. It is possible that this characteristic may be related to known climate oscillations such as the North Atlantic Oscillation, or the Arctic Oscillation, however, the details of these relationships – their temporal and spatial nature require further investigation.

Acknowledgements

This research was supported by NASA's Polar Program. The authors would like to thank Mr. Stephen Fiegles for systems support.

References

Abdalati W., and K. Steffen, Passive microwave-derived snow melt regions on the Greenland ice sheet, Geophys. Res. Lett., 22, 787-790.

Abdalati, W. and K. Steffen, Snow melt on the Greenland ice sheet as derived from passive microwave satellite data, *J. Clim., 10,* 165-175, 1997a.

Abdalati, W., and K. Steffen, The apparent effects of the Mt. Pinatubo eruption on the Greenland ice sheet melt extent, *Geophys. Res. Lett., 24*, 1795-1797, 1997b.

Abdalati, W.,W. Krabill, E. Frederick, S. Manizade, C. Martin, J. Sonntag, R. Swift, R. Thomas, W. Wright, and J. Yungel, Outlet glacier and margin elevation changes: near coastal thinning of the Greenland ice sheet, *J. Geophys. Res. Atmos.*, submitted.

Bluth, G.J.S., S.D. Doiron, C.C. Schnetzler, A.J. Krueger, and L.S. Walter, Global tracking of the SO_2 clouds from the June 1991 Mt. Pinatubo eruptions, *Geophys. Res. Lett., 19*, 151-154, 1992.

Jezek, K.C., C. Merry, D. Cavalieri, S. Grace, J. Bedner, D. Wilson, and D. Lampkin, 1991. Comparison between SMMR and SSM/I passive microwave data collected over the

Antarctic ice sheet, *Byrd Polar Research Center Technical Report No. 91-03*, 62 pp., The Ohio State University, Columbus, Ohio, 1991.

Krabill, W. W. Abdalati, E. Frederick, S. Manizade, C. Martin, J. Sonntag, R. Swift, R. Thomas, W. Wright, and J. Yungel, Greenland ice sheet: high-elevation balance and peripheral thinning, *Science*, in press.

Krabill, W., E. Frederick, S. Manizade, C. Martin, J. Sonntag, R. Swift, R. Thomas, W. Wright, J. Yungel, Rapid thinning of parts of the southern Greenland ice sheet, *Science. 283*, 1522-1524, 1999

Matzler, C.H., and R. Huppi, Review of signature studies for microwaveremote sensing of snowpacks, *Adv. In Space Res., 9*, 253-265, 1989.

McCormick, M.P., T.J. Swissler, W.H. Fuller, W.H. Hunt, and M.T. Osborn, Airborne and ground-based lidar measurements of the El Chichon stratospheric aerosol from 90°N to 56°S, *Geofis. Int., 33*, 187-221, 1984.

Mote, T.L., M.R. Anderson, K.C. Kuivinen, and C.M. Rowe, Passive microwave-derived spatial and temporal variations of summer melt on the Greenland ice sheet. *Ann Glaciol., 17*, 233-238, 1993.

Mote T.L., and M.R. Anderson, Variations in snowpack melt on the Greenland ice sheet based on passive-microwave measurements. *J. Glaciol., 41,* 51-60, 1995.
Paterson, W.B., *The Physics of Glaciers*, 480 pp., Elsevier Science Ltd. Oxford, 1994.

Ohmura, A., and N. Reeh, New precipitation and accumulation maps for Greenland. *J. Glaciol., 37*, 140-148, 1991.

Post, .M.J., C.J. Grund, A.M. Weickmann, K.R. Healy, and R.J. Willis, Comparison of Mt. Pinatubo and El Chichon volcanic events, *J. Geophys. Res., 101*, 3929-3940, 1996.

Robin, G. de Q., Depth of water-filled crevasses that are closely spaced, *J. Glaciol., 13*, 543, 1974.

Stone, R.S., J.R. Key, and E.G. Dutton, Properties and decasy of stratospheric aerosols in the Arctic, *Geophys. Res. Lett., 20*, 2639-2642, 1993.

Stroeve J., J. Maslanik, and X.M. Li., An intercomparison of DMSP F11- and F13-derived sea ice products, *Remote Sens. Environ., 64*, 132-152, 1998.

Thomas, R.H., W. Abdalati, T.L. Akins, B.M. Csatho, E.B. Frederick, S.P. Gogineni, W.B. Krabill, S.S. Manizade, E.J. Rignot, Substantial thinning of a major east Greenland outlet glacier, *Geophys. Res. Lett., 27*, 1291-1294, 2000.

Ulaby, F.T, R.K. Moore, and A.K. Fung, Microwave Remote Sensing. Vol. 3, From Theory to Applications, 1120 pp., 1986.

Van der Veen, C.J., Fracture mechanics approach to penetration of surface crevasses on glaciers. *Cold Regions Sci. Tech.*, *27*, 31-47, 1998

Warrick, R. C. Le Provost, M. Meier, J. Oerlemans, P. Woodworth, in Climate Change, 1995: The Science of Climate Change, edited by, ????? pp. 359-405. Cambridge University Press, Cambridge, 1996

Zwally. H.J., and S. Fiegles, Extent and duration of Antarctic surface melting, *J. Glaciol.*, *40*, 463-476, 1994.

Figure Captions:

Figure 1. The Greenland ice sheet. The gray interior shows the areas used in the ice mask, and coastal stations from which temperature averages were determined are shown as well. Temperatures from the three stations in the southwest were averaged to avoid a regional bias.

Figure 2. 1979-1999 mean melt extent (average melt area for June, July, and August), for different climate zones on the ice sheet as defined by Ohmura and Reeh [1991]. Melt conditions in the west, show a significant increasing trend, while those on the east either negligible or negative trends.

Figure 3. 1979-1999 mean melt extent for the entire ice sheet. Also shown are average temperature anomalies for the time period for the six coastal stations shown in Fig. 1. The melt shows an increasing trend of 0.97%/yr at the 88% significance level. This coincides with a warming of 0.24°C over the 21-year period. The correlation coefficient between melt and temperature is R=0.82.

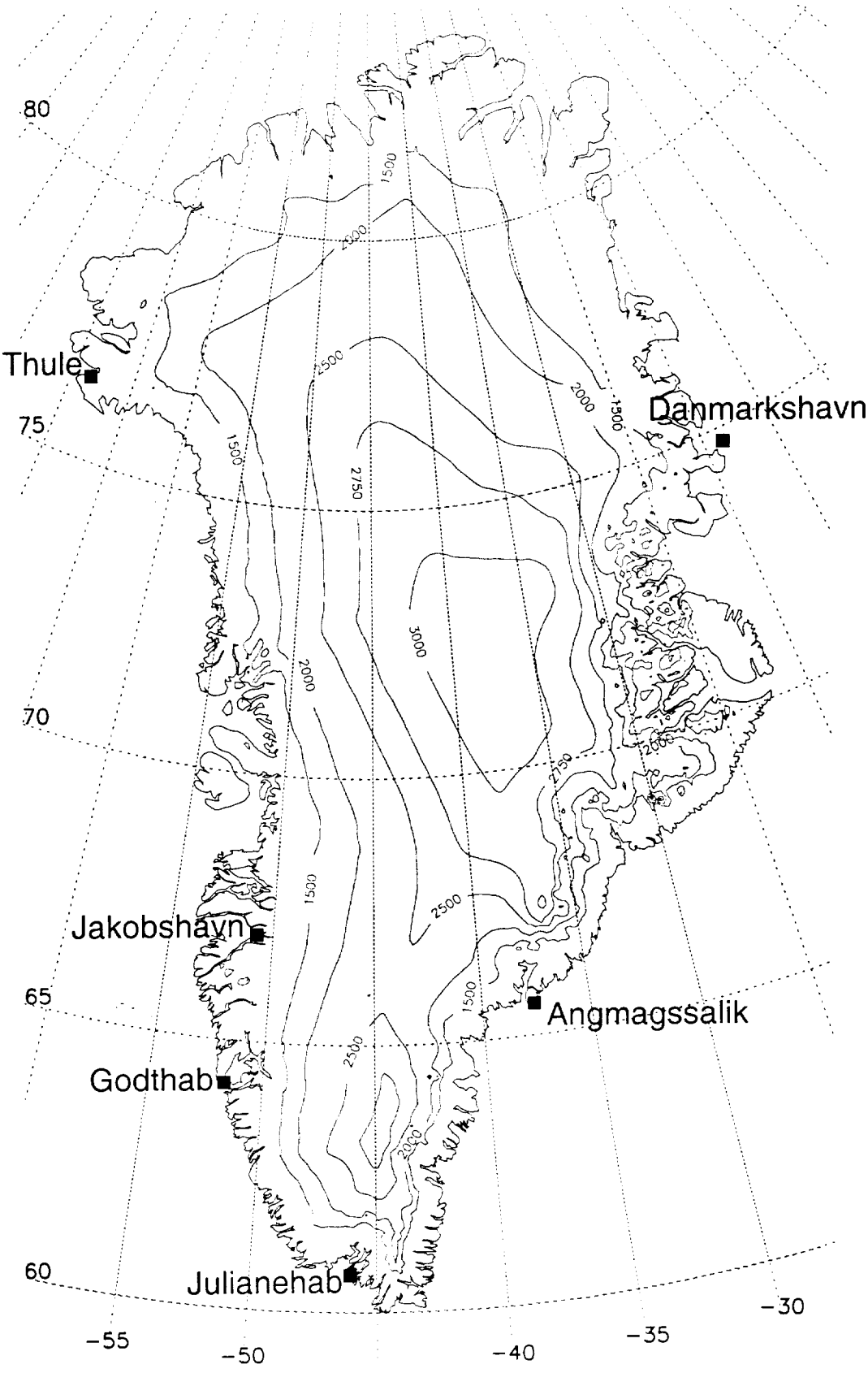
80
75
70
65
60
−55
−50
−40
−35
−30
Thule
Danmarkshavn
Jakobshavn
Angmagssalik
Godthab
Julianehab
1500
2000
2500
3000
2750

Fig. 1

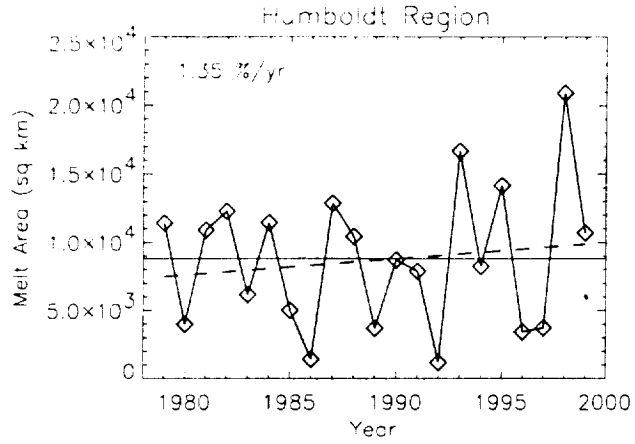

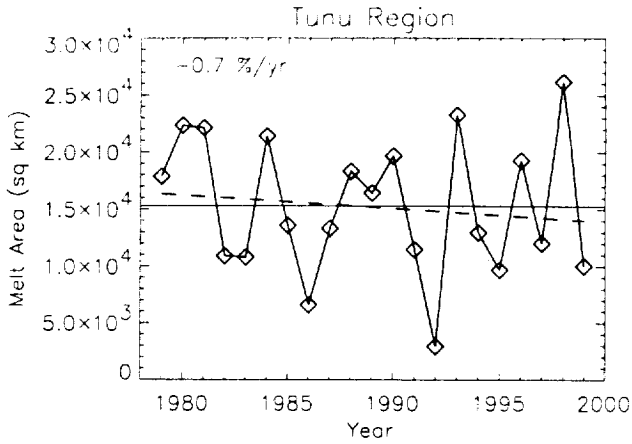

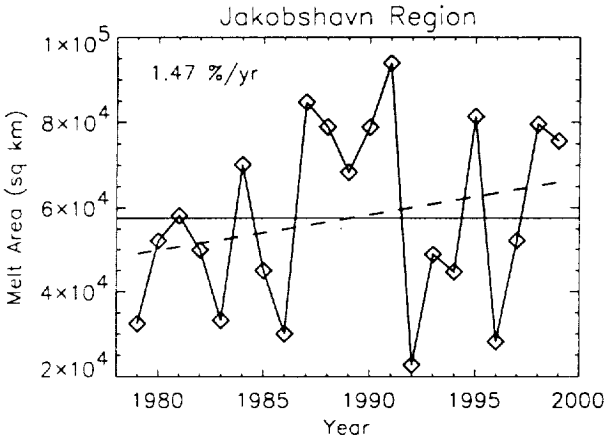

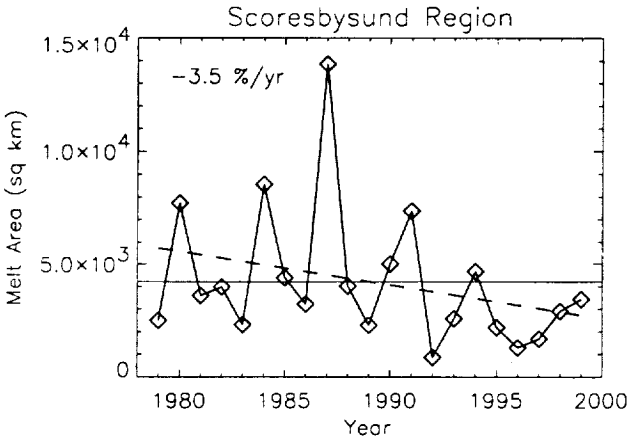

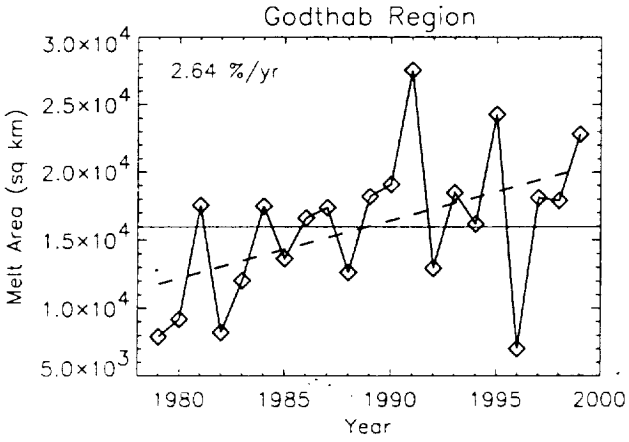

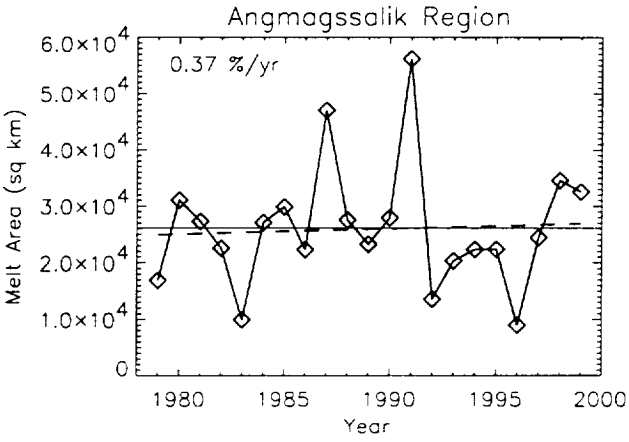

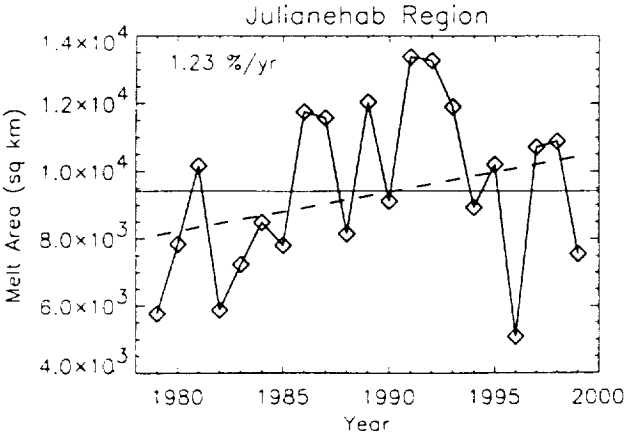

Place Figure 2 Insert Here

Fig 2

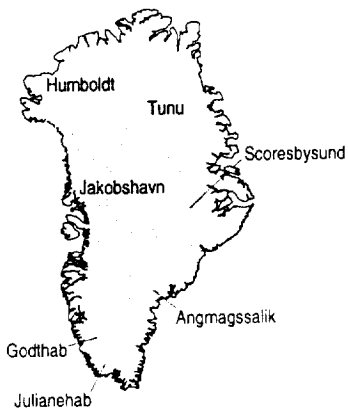

Figure insert

Fig. 2 insert

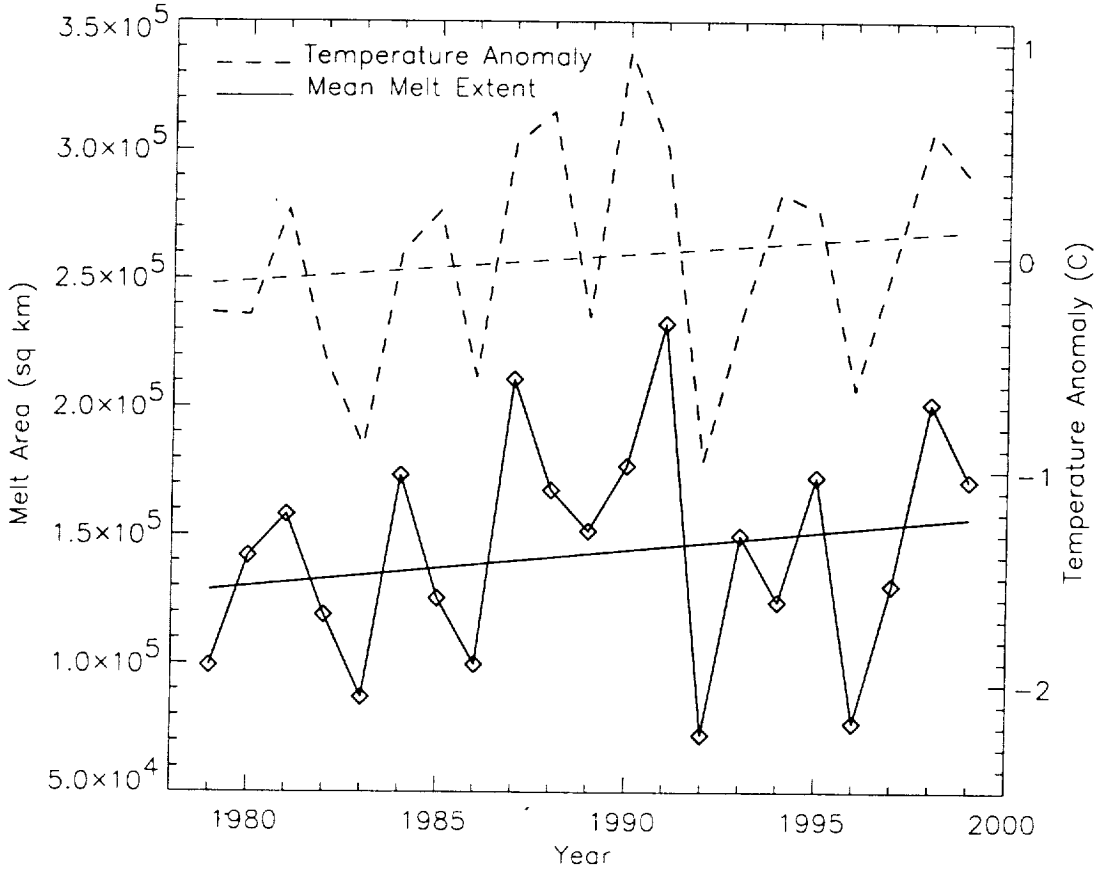
Temperature Anomaly
Mean Melt Extent
Melt Area (sq km)
Temperature Anomaly (C)
Year
3.5×10^5
3.0×10^5
2.5×10^5
2.0×10^5
1.5×10^5
1.0×10^5
5.0×10^4
1
0
−1
−2
1980
1985
1990
1995
2000

Fig. 3